Maximally-localized Wannier functions in perovskites: Cubic $BaTiO_3$

Nicola Marzari and David Vanderbilt

Department of Physics and Astronomy, Rutgers University, Piscataway, NJ 08854-8019

Abstract. The electronic ground state of a periodic crystalline solid is usually described in terms of extended Bloch orbitals; localized Wannier functions can alternatively be used. These two representations are connected by families of unitary transformations, carrying a large degree of arbitrariness. We have developed a localization algorithm that allows one to iteratively transform the extended Bloch orbitals of a first-principles calculation into a unique set of *maximally localized* Wannier functions. We apply this formalism here to the case of cubic $BaTiO_3$. The purpose is twofold. First, a localized-orbital picture allows a meaningful band-by-band decomposition of the whole Bloch band complex. In perovskites, these Wannier functions are centered on the atomic sites and display clearly a s, p, d, or hybrid character. Second, since the centers of the Wannier functions map the polarization field onto localized point charges, the ground state dielectric properties become readily available. We study the Born effective charges of the paraelectric phase of $BaTiO_3$. We are able to identify not only the contributions that come from a given group of bands, but also the individual contributions from the "atomic" Wannier functions that comprise each of these groups.

INTRODUCTION

The electronic ground state of a periodic solid, in the independent particle approximation, is naturally labelled according to the prescriptions of Bloch's theorem: single-particle orbitals are assigned a quantum number $\mathbf{k}$ for the crystal momentum, together with a band index n. Although this choice is widely used in electronic structure calculations, alternative representations are available. The Wannier representation [1], essentially a real-space picture of localized orbitals, assigns as quantum numbers the lattice vector $\mathbf{R}$ of the cell where the orbital is localized, together with the band index n. Wannier functions can be a powerful tool in the study of the electronic and dielectric properties of materials: they are the solid-state equivalent of "localized molecular orbitals" [2], and thus provide an insightful picture of the nature of chemical bonding, otherwise missing from the Bloch picture of extended orbitals. In addition, the modern theory of polarization [3] directly relates the centers of the Wannier functions to the macroscopic polarization of a crystalline insulator.

Wannier functions are strongly non-unique. This is a consequence of the phase indeterminacy $e^{i\phi_n(\mathbf{k})}$ that Bloch orbitals $\psi_{n\mathbf{k}}$ have at every wavevector $\mathbf{k}$. This indeterminacy is actually more general than just the phase factors: Bloch orbitals belonging to a composite group of bands (i.e. bands that are connected between themselves by degeneracies, but separated from others by energy gaps) can undergo arbitrary unitary transformations $U^{(\mathbf{k})}$ between themselves at every $\mathbf{k}$. We have recently developed a procedure [4] that can iteratively refine these otherwise arbitrary degrees of freedom, so that they lead to Wannier functions that are well defined and that are localized around their centers (in particular, they minimize the second moment around the centers). Such a procedure can be applied either to a whole band complex of Bloch orbitals, or just to some isolated subgroups.

As a natural first application of this technique, we present here results for the case of $BaTiO_3$ in the cubic phase. Perovskite ferroelectrics, of which $BaTiO_3$ is a paradigmatic example, owe their very rich phenomenology to the subtle competition of several degrees of freedom, balancing the long-range dipole-dipole interaction with short-range Pauli repulsion. One of the striking features is the display of anomalously large Born effective charges [5]. Their origin is understood in a simple tight-binding picture [6]: the change in the bond length (Ti-O in this case) corresponds to a dynamic charge transfer that is stronger when the bonding is borderline between ionic and covalent. Localized Wannier functions can thus be used to investigate the nature of this bonding, and to monitor the changes that follow a ferroelectric distortion. Additionally, the displacement of each Wannier center relates directly to the effective charge contribution of its orbital, and can be used to identify the nominal and the anomalous contributions to the polarization induced by an atomic displacement.

METHOD

Electronic structure calculations are carried out using periodic boundary conditions. This is the most natural choice to study perfect crystals and to minimize finite size-effects in the study of several non-periodic systems (e.g. surfaces, or impurities). The one-particle effective Hamiltonian $\hat{H}$ then commutes with the lattice-translation operator $\hat{T}_{\mathbf{R}}$, allowing one to choose as common eigenstates the Bloch orbitals $|\,\psi_{n\mathbf{k}}\,\rangle$,

$$[\,\hat{H},\,\hat{T}_{\mathbf{R}}\,] \;=\; 0 \;\;\Rightarrow\;\; \psi_{n\mathbf{k}}(\mathbf{r}) \;=\; e^{i\phi_n(\mathbf{k})}\,u_{n\mathbf{k}}(\mathbf{r})\,e^{i\mathbf{k}\cdot\mathbf{r}} \quad , \tag{1}$$

where $u_{n\mathbf{k}}(\mathbf{r})$ has the periodicity of the Hamiltonian. There is an arbitrary phase $\phi_n(\mathbf{k})$, periodic in reciprocal space, that is not assigned by the Schrödinger equation and that we have written out explicitly. We obtain a (non-unique) Wannier representation using any unitary transformation of the form $\langle\, n\mathbf{k}\,|\,\mathbf{R}n\,\rangle = e^{i\varphi_n(\mathbf{k})\,-i\mathbf{k}\cdot\mathbf{R}}$:

$$|\,\mathbf{R}n\,\rangle \;=\; \frac{V}{(2\pi)^3}\int_{BZ} |\,\psi_{n\mathbf{k}}\,\rangle\, e^{i\varphi_n(\mathbf{k})\,-i\mathbf{k}\cdot\mathbf{R}}\,d\mathbf{k} \quad . \tag{2}$$

Here V is the real-space primitive cell volume. It is easily shown that the $|\,\mathbf{R}n\,\rangle$ form an orthonormal set, and that two Wannier functions $|\,\mathbf{R}n\,\rangle$ and $|\,\mathbf{R}'n\,\rangle$ transform into each other with a translation of a lattice vector $\mathbf{R}-\mathbf{R}'$ [7]. The arbitrariness that is present in $\varphi_n(\mathbf{k})$ [or $\phi_n(\mathbf{k})$] propagates to the resulting Wannier functions, making the Wannier representation non-unique. Since the electronic energy functional in an insulator is also invariant with respect to a unitary transformation of its n occupied Bloch orbitals, there is additional freedom associated with the choice of a full unitary matrix (and not just a diagonal one) transforming the orbitals between themselves at every wavevector $\mathbf{k}$. Thus, the most general operation that transforms the Bloch orbitals into Wannier functions is given by

$$|\,\mathbf{R}n\,\rangle \;=\; \frac{V}{(2\pi)^3}\int_{BZ}\sum_m U_{mn}^{(\mathbf{k})}\,|\,\psi_{m\mathbf{k}}\,\rangle\,e^{-i\mathbf{k}\cdot\mathbf{R}}\,d\mathbf{k}\quad . \tag{3}$$

The Wannier functions $w_n(\mathbf{r}-\mathbf{R})=|\,\mathbf{R}n\,\rangle$, for non-pathological choices of phases, are "localized": for a $\mathbf{R}_i$ far away from $\mathbf{R}$, $w_n(\mathbf{R}_i-\mathbf{R})$ is a combination of terms like $\int_{BZ}\;u_{m\mathbf{k}}(0)e^{i\mathbf{k}\cdot(\mathbf{R}_i-\mathbf{R})}\,d\mathbf{k}$, which are small due to the rapidly varying character of the exponential factor [7].

Maximally-localized Wannier functions

Several heuristic approaches have been developed that construct reasonable sets of Wannier functions, reducing the arbitrariness in the $U_{mn}^{(\mathbf{k})}$ with symmetry considerations and analiticity requirements [8], or explicitly employing projection techniques on the occupied subspace spanned by the Bloch orbitals [9]. At variance with those approaches, we introduce a well-defined *localization criterion*, choosing the functional

$$\Omega=\sum_n\left[\langle r^2\rangle_n-\bar{\mathbf{r}}_n^{\,2}\right] \tag{4}$$

as the measure of the spread of the Wannier functions. The sum runs over the n functions $|\,\mathbf{0}n\,\rangle$; $\langle r^2\rangle_n$ and $\bar{\mathbf{r}}_n=\langle\mathbf{r}\rangle_n$ are the expectation values $\langle\,\mathbf{0}n\,|\,r^2\,|\,\mathbf{0}n\,\rangle$ and $\langle\,\mathbf{0}n\,|\,\mathbf{r}\,|\,\mathbf{0}n\,\rangle$. Given a set of Bloch orbitals $|\,\psi_{m\mathbf{k}}\,\rangle$, the goal is to find the choice of $U_{mn}^{(\mathbf{k})}$ in (3) that minimizes the values of the localization functional (4). We are able to express the gradient $G=\frac{d\Omega}{dW}$ of the localization functional with respect to an infinitesimal unitary rotation of our set of Bloch orbitals

$$|u_{n\mathbf{k}}\rangle\;\rightarrow\;|u_{n\mathbf{k}}\rangle+\sum_m dW_{mn}^{(\mathbf{k})}\,|u_{m\mathbf{k}}\rangle\quad , \tag{5}$$

where dW an infinitesimal antiunitary matrix $dW^\dagger=-dW$ such that

$$U_{mn}^{(\mathbf{k})}=\delta_{mn}+dW_{mn}^{(\mathbf{k})}\quad . \tag{6}$$

This provides an equation of motion for the evolution of the $U_{mn}^{(\mathbf{k})}$, and of the $|\,\mathbf{R}n\,\rangle$ derived in (3), towards the minimum of Ω; small finite steps in the direction opposite to the gradient decrease the value of Ω, until a minimum is reached.

1 Real-space representation

There are several interesting consequences stemming from the choice of (4) as the localization functional, that we briefly summarize here. Adding and subtracting the off-diagonal components $\widetilde{\Omega} = \sum_n \sum_{\mathbf{R}m\neq\mathbf{0}n} \left|\langle \mathbf{R}m|\mathbf{r}|\mathbf{0}n\rangle\right|^2$, we obtain the decomposition $\Omega = \Omega_{\rm I} + \Omega_{\rm D} + \Omega_{\rm OD}$, where $\Omega_{\rm I}$, $\Omega_{\rm D}$ and $\Omega_{\rm OD}$ are respectively

$$\Omega_{\rm I} = \sum_n \left[\langle r^2 \rangle_n - \sum_{\mathbf{R}m} \left|\langle \mathbf{R}m|\mathbf{r}|\mathbf{0}n\rangle\right|^2 \right] ,$$

$$\Omega_{\rm D} = \sum_n \sum_{\mathbf{R}\neq\mathbf{0}} \left|\langle \mathbf{R}n|\mathbf{r}|\mathbf{0}n\rangle\right|^2 ,$$

$$\Omega_{\rm OD} = \sum_{m\neq n} \sum_{\mathbf{R}} \left|\langle \mathbf{R}m|\mathbf{r}|\mathbf{0}n\rangle\right|^2 .$$

It can be shown that all terms are *positive-definite* (in particular $\Omega_{\rm I}$, see Ref. [4]); more importantly, $\Omega_{\rm I}$ is also *gauge-invariant*, i.e., it is invariant under any arbitrary unitary transformation (3) of the Bloch orbitals. The minimization procedure thus corresponds to the minimization of $\widetilde{\Omega} = \Omega_{\rm D} + \Omega_{\rm OD}$. At the minimum, the elements $\left|\langle \mathbf{R}m|\mathbf{r}|\mathbf{0}n\rangle\right|^2$ are as small as possible, realizing the best compromise in the simultaneous diagonalization, within the space of the Bloch bands considered, of the three position operators x, y and z (which do not in general commute when projected within this space).

2 Reciprocal-space representation

As shown by Blount [7], matrix elements of the position operator between Wannier functions take the form

$$\langle \mathbf{R}n|\mathbf{r}|\mathbf{0}m\rangle = i\,\frac{V}{(2\pi)^3} \int d\mathbf{k}\, e^{i\mathbf{k}\cdot\mathbf{R}} \langle u_{n\mathbf{k}}|\nabla_{\mathbf{k}}|u_{m\mathbf{k}}\rangle \tag{7}$$

and

$$\langle \mathbf{R}n|r^2|\mathbf{0}m\rangle = -\frac{V}{(2\pi)^3} \int d\mathbf{k}\, e^{i\mathbf{k}\cdot\mathbf{R}} \langle u_{n\mathbf{k}}|\nabla^2_{\mathbf{k}}|u_{m\mathbf{k}}\rangle \quad . \tag{8}$$

These expressions provide the needed connection with our underlying Bloch formalism, since they allow us to express the localization functional Ω in terms of the matrix elements of $\nabla_{\mathbf{k}}$ and $\nabla^2_{\mathbf{k}}$. We thus determine the Bloch orbitals $|u_{m\mathbf{k}}\rangle$ on a regular mesh of $\mathbf{k}$-points, and use finite differences to evaluate the above derivatives. For any given $\mathbf{k}$-point in a regular cubic mesh (sc, fcc, bcc), we have a star $\mathbf{b}$ of Z $\mathbf{k}$-points that are first-neighbors; their weights in the evaluation of derivatives are $w_b = 3/Zb^2$. We define $M^{(\mathbf{k},\mathbf{b})}_{mn} = \langle u_{m\mathbf{k}}|u_{n,\mathbf{k}+\mathbf{b}}\rangle$ as the matrix elements

between Bloch orbitals at neighboring **k**-points. The $M_{mn}^{(\mathbf{k},\mathbf{b})}$ are a central quantity in our formalism, since we can then express all the contributions to the localization functional using the connection made by Blount, together with our finite-difference evaluations of the gradients. After some algebra we obtain [4]

$$\Omega_{\rm I} = \frac{1}{N}\sum_{\mathbf{k},\mathbf{b}} w_b \left(N_{\rm bands} - \sum_{mn} |M_{mn}^{(\mathbf{k},\mathbf{b})}|^2 \right) , \tag{9}$$

$$\Omega_{\rm OD} = \frac{1}{N}\sum_{\mathbf{k},\mathbf{b}} w_b \sum_{m\neq n} |M_{mn}^{(\mathbf{k},\mathbf{b})}|^2 , \tag{10}$$

and

$$\Omega_{\rm D} = \frac{1}{N}\sum_{\mathbf{k},\mathbf{b}} w_b \sum_{n} \left(-{\rm Im}\ln M_{nn}^{(\mathbf{k},\mathbf{b})} - \overline{{\rm Im}\ln M_{nn}^{(\mathbf{k},\mathbf{b})}} \right)^2 . \tag{11}$$

From these, we can calculate the change in the localization functional in response to an infinitesimal unitary transformation of the Bloch orbitals, as a function of the $M_{mn}^{(\mathbf{k},\mathbf{b})}$; once these steepest-descents are available, it is straightforward to construct a procedure that updates the $U_{mn}^{(\mathbf{k})}$ towards the minimum of the functional.

RESULTS: THE CASE OF $BATIO_3$

We study here the cubic phase of $BaTiO_3$, using a plane-wave total-energy pseudopotential approach with the local-density approximation to the exchange-correlation functional. We use norm-conserving pseudopotentials in the Kleinman-Bylander representation, with q_c kinetic-energy tuning [10] for the oxygen atom and a Troullier-Martins procedure [11] for the titanium, to bring the cutoff convergence down to 900 eV. The $3s$ and $3p$ levels of titanium have been included in the valence. The Brillouin zone is sampled with a $4 \times 4 \times 4$ Monkhorst-Pack mesh; the lattice parameter used is 3.98Å.

Wannier functions of cubic $BaTiO_3$

The minimization of the total energy provides the Kohn-Sham Bloch orbitals on a regular mesh of **k**-points, that are then used as a starting point for the construction of the Wannier functions. The subsequent minimization of the localization functional determines the $U_{mn}^{(\mathbf{k})}$ that correspond to the maximally-localized Wannier functions. In $BaTiO_3$ there are several groups of bands that are separated by gaps. In order of increasing energy, we have the band groups corresponding to the Ti $3s$ (1), Ti $3p$ (3), Ba $5s$ (1), O $2s$ (3), Ba $5p$ (3) and O $2p$ (9) levels (in parenthesis are the number of bands in each group). We initially consider each group of

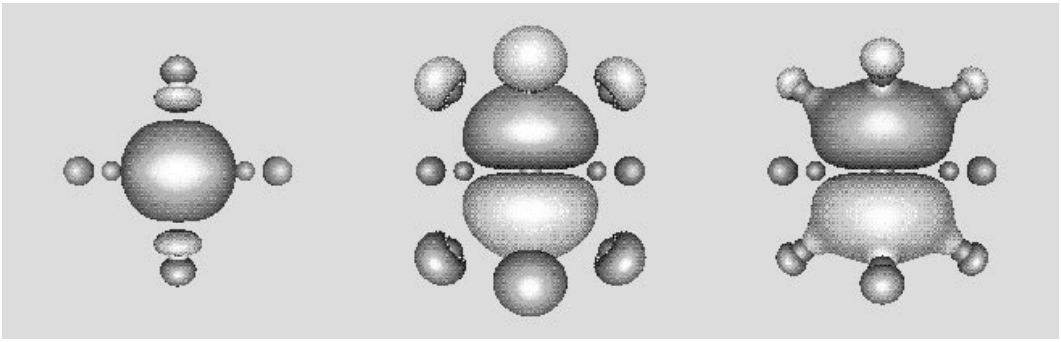

FIGURE 1. Left panel: oxygen-centered Wannier function from the O $2s$ 3-band group (the O atom is surrounded by four Ba atoms on the sides, and two Ti atoms on top and bottom). Center and right panels: barium-centered Wannier function from the Ba $5p$ 3-band group, and barium-centered Wannier function from the Ba $5p$ and the O $2s$ 6-band group (the Ba atom is surrounded by 12 oxygens).

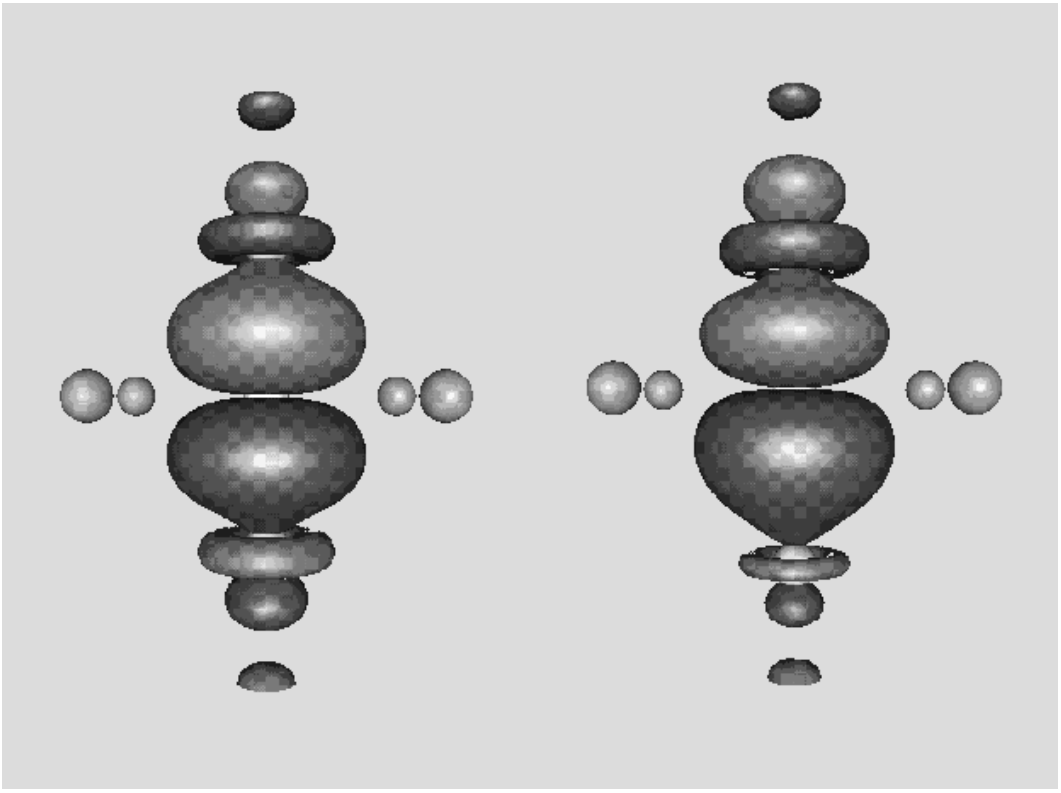

FIGURE 2. Oxygen-centered σ Wannier function from the localization of the O $2p$ 9-band group. The orbital is oriented along the Ti-O-Ti bond; the four Ba atoms neighboring the central oxygen and the two Ti atoms on top and bottom are also shown. Left panel: ideal atomic positions. Right panel: same, but with the titanium atoms displaced downwards.

bands separately, and perform the minimization on the 6 subspaces of dimensions 1×1, 3×3, 1×1, 3×3, 3×3, and 9×9.

The Wannier functions determined from the the Ti $3s$ or the Ti $3p$ groups strongly resemble atomic orbitals, slightly deformed by the underlying crystal potential, and are not shown here. We show instead in the left panel of Fig. 1 one of the three oxygen-centered Wannier functions that are derived from the oxygen $2s$ bands. In each unit cell there are three such functions, sitting on each of the oxygens. The orbital shows its atomic s character; there are some contributions on the Ti, with p and/or d character (the titanium is slightly embedded in a d_{z^2} orbital). Interesting results emerge from the localization of the Ba $5p$ bands (Fig. 1, center and right panels). These bands correspond to three orbitals in each unit cell, all centered on the barium and oriented along the three cristallographic directions (p_x, p_y and p_z). It can easily be seen (center panel) that, in addition to the distinctive atomic p orbital on the barium, there are significant sp-like contributions sitting on 8 of the 12 neighboring oxygens. This supports the suggestion that barium in this compound has some covalent character [12], and it is consistent with the anomalous effective-charge contributions that come from this group of Wannier functions (see next subsection). It is interesting to note that if we decide to treat the Ba $5p$ bands together with the O $2s$ bands, we can (obviously) increase the degree of localization of each orbital. In this latter case (right panel) the sp contributions on the oxygens decrease, being transferred to the $2s$ orbitals localized on the oxygens themselves.

Finally, we examine the 9 oxygen $2p$ bands that result from the hybridization of the O $2p$ electrons with the Ba $6s$ and the Ti $4s$ and $3d$. There are three localized orbitals on each oxygen, oriented along the Ti-O-Ti bonds. We label two of these orbitals as π and one as σ, according to their symmetry along the Ti-O-Ti axis. One of the σ orbitals is shown in Fig. 2, first with the atoms in their ideal positions (left panel) and then with the Ti atoms displaced along the Ti-O bond (right panel). The σ orbital shows clearly the hybridization between the oxygen p orbital oriented along the Ti-O-Ti direction and the d_{z^2} orbital of the titanium. The σ and even more the π orbitals have strong anomalous contributions to the effective charges, that can be visualized with the large charge transfer from the oxygen atoms in response to the titanium displacements.

Band-by-band decomposition of the Born effective charges

The Born dynamical effective charges describe the change in macroscopic polarization that is induced by the displacement of a given ion. As such, they play a fundamental role in determining the dynamical properties of insulating crystals, and are a powerful tool to investigate the dielectric and ferroelectric properties of materials. They also determine the splitting of the infrared-active optical modes; in simpler compounds (e.g. GaAs) they can be unambiguously determined from the experimental phonon dispersions. Perovskite ferroelectrics display anomalous, large effective charges, that can be almost double their nominal ionic value. The

TABLE 1. Born effective charges decomposed into atomic contributions, for $BaTiO_3$. The $Z^{\star}_{el}$ are calculated by displacing a Ba, Ti or a O sublattice (O_1 is parallel to the Ti-O direction, O_2 perpendicular) by δa_0, where $\delta = 0.002$. The numbers in parenthesis are those of Ghosez et al. (a_0=3.94Å). Horizontal lines group band complexes that have been treated together in the Wannier minimization. Top line in each group is the total for that group. We have added at the bottom the O $2p$ decomposition obtained in a calculation performed using a Ti atom with the $3s$ and $3p$ levels frozen in the core (Ti^{4+}).

	Ba $(\delta,0,0)$		Ti $(\frac{1}{2}+\delta,\frac{1}{2},\frac{1}{2})$		O_1 $(\frac{1}{2},\frac{1}{2},\delta)$		O_2 $(\frac{1}{2}+\delta,\frac{1}{2},0)$	
Ti $3s$ (1)	0.01	(0.01)	-2.04	(-2.03)	0.03	(0.02)	0.00	(0.00)
Ti $3p$ (3)	0.02	(0.02)	-6.19	(-6.22)	0.21	(0.21)	-0.02	(-0.02)
$(\frac{1}{2},\frac{1}{2},\frac{1}{2})$	0.00		-2.21		0.00		0.00	
$(\frac{1}{2},\frac{1}{2},\frac{1}{2})$	0.01		-1.99		0.21		-0.02	
$(\frac{1}{2},\frac{1}{2},\frac{1}{2})$	0.01		-1.99		0.00		0.00	
Ba $5s$ (1)	-2.09	(-2.11)	0.04	(0.05)	0.01	(0.01)	0.02	(0.02)
O $2s$ (3O)	0.65	(0.73)	0.20	(0.23)	-2.45	(-2.51)	-2.21	(-2.23)
$(0,\frac{1}{2},\frac{1}{2})$	-0.11		0.48		-0.04		-0.01	
$(\frac{1}{2},0,\frac{1}{2})$	0.38		-0.14		-0.04		0.01	
$(\frac{1}{2},\frac{1}{2},0)$	0.38		-0.14		-2.36		-2.21	
Ba $5p$ (3Ba)	-7.20	(-7.38)	0.31	(0.36)	-0.11	(-0.13)	0.50	(0.58)
$(0,0,0)$	-2.46		0.04		-0.06		0.21	
$(0,0,0)$	-2.37		0.14		0.01		0.01	
$(0,0,0)$	-2.37		0.14		-0.06		0.29	
O $2p$ (9)	1.26	(1.50)	3.01	(2.86)	-9.57	(-9.31)	-6.35	(-6.50)
$(0,\frac{1}{2},\frac{1}{2})\sigma$	-0.01		0.81		-0.07		0.03	
$(0,\frac{1}{2},\frac{1}{2})\pi$	-0.20		1.78		-0.17		-0.49	
$(0,\frac{1}{2},\frac{1}{2})\pi$	-0.20		1.78		-0.01		0.00	
$(\frac{1}{2},0,\frac{1}{2})\pi$	0.22		-0.17		-0.01		0.01	
$(\frac{1}{2},0,\frac{1}{2})\pi$	0.51		-0.27		-0.17		0.04	
$(\frac{1}{2},0,\frac{1}{2})\sigma$	0.10		-0.24		-0.07		0.02	
$(\frac{1}{2},\frac{1}{2},0)\pi$	0.22		-0.17		-3.10		-1.89	
$(\frac{1}{2},\frac{1}{2},0)\sigma$	0.10		-0.24		-2.86		-1.81	
$(\frac{1}{2},\frac{1}{2},0)\pi$	0.51		-0.27		-3.10		-2.26	
Total $Z^{\star}_{el}$	-7.35		-4.67		-11.87		-8.06	
Core	10.00		12.00		6.00		6.00	
Total $Z^{\star}$	2.65	(2.77)	7.33	(7.25)	-5.87	(-5.71)	-2.06	(-2.15)
Ref. [5]	2.75		7.16		-5.69		-2.11	
Ti^{4+}								
O 2p (9)	1.29	(1.50)	2.33	(2.86)	-8.93	(-9.31)	-6.36	(-6.50)
$(0,\frac{1}{2},\frac{1}{2})\sigma$	-0.02		0.49		-0.13		0.01	
$(0,\frac{1}{2},\frac{1}{2})\pi$	-0.19		1.48		-0.19		-0.41	
$(0,\frac{1}{2},\frac{1}{2})\pi$	-0.19		1.48		-0.02		-0.01	
$(\frac{1}{2},0,\frac{1}{2})\pi$	0.22		-0.16		-0.02		0.01	
$(\frac{1}{2},0,\frac{1}{2})\pi$	0.51		-0.25		-0.19		0.04	
$(\frac{1}{2},0,\frac{1}{2})\sigma$	0.11		-0.15		-0.13		0.03	
$(\frac{1}{2},\frac{1}{2},0)\pi$	0.22		-0.16		-2.88		-1.89	
$(\frac{1}{2},\frac{1}{2},0)\sigma$	0.11		-0.15		-2.50		-1.87	
$(\frac{1}{2},\frac{1}{2},0)\pi$	0.51		-0.25		-2.88		-2.28	

origin of this effect lies in the large dynamical charge transfer that takes place when moving away from the high-symmetry cubic phase (i.e., going from more ionic to more covalent bonding). Orbital hybridization is necessary for this transfer to take place; for this reason, our localized-orbitals approach provides an insightful tool in examining these effects. In the language of the modern thory of polarization [3], the anomalous contribution is determined by the relative displacement of the Wannier centers with respect to the ion that is being moved. If the bonding were purely ionic, electrons (and thus Wannier centers) would be firmly localized on each anion, and move rigidly with it. This is not the case in perovskite oxides. The anomalous contribution is often traced [13] to substantial hybridization between the oxygen p orbitals and the d orbitals of the atom in the B site (Ti, in this case). The picture can be somewhat more complex, with other group of bands playing a role in the anomalous dielectric behavior.

We present in Table 1 a full decomposition of the effective charges in $BaTiO_3$ coming from the different groups of bands; and, inside each group, coming from the individual Wannier functions identified by the localization procedure. We compare the results for the groups of bands with those obtained by Ghosez et al. (Ref. [12]). We find very good agreement, given the difference in the pseudopotentials used and our choice of lattice parameter. These results underline the conclusion that the decomposition into band groups is consistently defined in the linear-response formalism only when the calculations are performed in the so-called *diagonal gauge* [12]. The effective-charge tensor reduces to a scalar for barium and titanium, while it is diagonal with two inequivalent components (those parallel and perpendicular to the Ti-O bonds) for the oxygens. Several facts stand out from an inspection of the table. The anomalous effective charges originate not only from the oxygen $2p$ bands; there are also sizeable contributions originating from the barium $5p$ orbitals and even from the oxygen $2s$. More notably, there is a wide range of *compensating effects* between groups of bands and between different orbitals inside each group. The partial cancellation of such large orbital polarizabilities hints again at the complexity of these materials, which exhibit such a wide range of equilibrium properties as a consequence of the existence of many of these competing effects. Titanium shows the strongest deviations from a naive ionic picture. The σ and π oxygen orbitals carry a *positive* electronic $Z^\star$ contribution, equal respectively to 0.81 and 1.78. It should be noted that it is always the O $2p$ π orbitals that carry the largest anomalous charge. The O $2p$ contributions to the O_1 effective charges (i.e. in the direction of the Ti-O bond) are also anomalous, up to -1.10 for each π orbital (in addition to the nominal -2.00 for each orbital).

Finally, we present at the bottom of Table 1 the oxygen $2p$ decomposition performed in a calculation where the $3s$ and $3p$ orbitals of the titanium have been removed from the pseudopotential (i.e., removed from the valence and frozen in the core). It is interesting to note that most contributions are completely unchanged; differences arise only for the anomalous contributions for the Ti and the O_1 displacements (whose anomality, incidentally, is reduced if this more approximate formalism is employed).

CONCLUSIONS

We have summarized here our formalism for obtaining maximally-localized Wannier functions from the Bloch orbitals of an ab-initio electronic structure calculation. This formalism can be very helpful in understanding the chemical and dielectric properties of materials. Perovskite ferroelectrics are a particularly promising class of systems to be studied, since the nature of the bonding and hybridization can have a striking influence on the dielectric properties and on the development of ferroelectricity. At variance with other approaches, our method allows for a decomposition of electronic properties (e.g., the effective charges) into meaningful atomic contributions. In the case of $BaTiO_3$, it elucidates in particular the origins of the large anomalous contributions to the effective charges.

ACKNOWLEDGMENTS

This work was supported by ONR Grant N00014-97-1-0048, and NSF Grants DMR-96-13648 and ASC-96-25885. We would like to thank Ph. Ghosez and X. Gonze for providing an early copy of their work on the effective-charge decompositions.

REFERENCES

1. G. H. Wannier, Phys. Rev. **52**, 191 (1937).
2. S. F. Boys, in *Quantum Theory of Atoms, Molecules, and the Solid State,* P.-O. Löwdin, ed. (Academic Press, New York, 1966), p. 253.
3. R. D. King-Smith and D. Vanderbilt, Phys. Rev. B **47**, 1651 (1993); R. Resta, Rev. Mod. Phys. **66**, 899 (1994).
4. N. Marzari and D. Vanderbilt, Phys. Rev. B **56**, 12847 (1997).
5. W. Zhong, R. D. King-Smith and D. Vanderbilt, Phys. Rev. Lett. **72**, 3618 (1994).
6. W. A. Harrison, *Electronic Structure and the Properties of Solids*, (Dover, New York, 1980).
7. E.I. Blount, Solid State Physics **13**, 305 (1962).
8. B. Sporkmann and H. Bross, J. Phys.: Condens. Matter **9**, 5593 (1997); H. Teichler, Phys. Stat. Sol. (b) **43**, 307 (1971); H. Bross, Z. Physik **243**, 311 (1971); B. Sporkmann and H. Bross, Phys. Rev. B **49**, 10869 (1994).
9. S. Satpathy and Z. Pawlowska, Phys. Stat. Sol. (b) **145**, 555 (1988); U. Stephan and D. A. Drabold, to be published.
10. M.-H. Lee, J.-S. Lin, M. C. Payne, V. Heine, V. Milman, and S. Crampin, to be published.
11. N. Troullier and J. L. Martins, Phys. Rev. B **43**, 1993 (1991).
12. Ph. Ghosez, X. Gonze, Ph. Lambin, and J.-P. Michenaud, Phys. Rev. B **51**, 6765 (1995); Ph. Ghosez and X. Gonze, to be published.
13. M. Posternak, R. Resta, and A. Baldereschi, Phys. Rev. B **50**, R8911 (1994).